Improvement of Compressible Vorticity Confinement Method by Combining It with Vortex Feature Detection Methods

M. Mohseni and S. M. Malek Jafarian[†]

Department of Mechanic Engineering, University of Birjand, Birjand, South Khorasan, Iran.

†Corresponding Author Email: mmjafarian@birjand.ac.ir

ABSTRACT

In the present study, the performance of the vorticity confinement method has been improved by combining it with the vortex feature detection methods. In the conventional vorticity confinement method, the only parameter to apply or not to apply vorticity confinement is the non-zero value of vorticity. On the other hand, the presence of vorticity in some cases, like the boundary layer and the shear layer flows, does not imply the presence of vortices. Applying the vorticity confinement at these points can lead to errors, in addition to loss of solution time. In order to solve this problem, using the combination of vorticity confinement method and four methods of vortex feature detection (non-dimensional Q, non-dimensional λ_2, non-dimensional modified Δ, and the $S - \Omega$ correlation) the vorticity confinement term is applied only in vortex regions. In order to investigate the effects of this combination, the compressible Euler equation has been investigated for the problem of two-dimensional stationary single vortex at Mach number 0.5. The results indicate significant positive effects in reducing the solving time, decreasing the sensitivity of the solution to the amount of confinement parameter and significant elimination of the oscillation.

Keywords: Threshold function; Confinement parameter; Vortex; Oscillations.

NOMENCLATURE

e_0	internal energy		v	velocity magnitude in y direction
E_c	confinement parameter		$\vec{V}$	velocity vector
$\vec{F}$	flux vector in x direction		$\vec{W}$	flow quantitative vector
$\vec{G}$	flux vector in y direction		$f_{threshold}$	threshold function
h_0	total energy		φ	vorticity magnitude
$\hat{n}$	unit vector perpendicular to the vortex line		ρ	density
p	pressure		γ	heat capacity ratio
$\vec{S}$	source term		ω	vorticity
u	velocity magnitude in x direction			

1. INTRODUCTION

Problems of vortex dominant flows have many applications in fluid mechanics, like the flow around skyscrapers, behind airplanes, etc. However, the numerical solution to these problems is facing a serious challenge. Due to the errors induced from the discretization of the equations, the vortices in the flow are diffused and dissipated at a higher rate than the reality, and this affects the validity of the results. To solve this problem, various solutions have been proposed, including using finer grids, adaptive grid solution, and the use of high order schemes for discretization. Despite the efficiency of these methods, their use is associated with increasing computational load and complexity of numerical codes. Furthermore, the vorticity confinement method presents a simple and low cost solution to solve this problem; this has led to an interesting topic on this research.

For the first time, Steinhoff *et al*., introduced the vorticity confinement methods for incompressible flows during 1992 to 1995 in

their researches (Steinhoff, 1994; Steinhoff *et al.*, 1994; Steinhoff and Raviprakash, 1995; Steinhoff *et al.*, 1992; Steinhoff *et al.*, 1995). In the solution proposed by Steinhoff, the error caused by the artificial viscosity was compensated by adding a source term to the momentum equation. After presenting the early papers on vorticity confinement, many attempts were made to extend this method to the compressible flows. In 1997, Pevchin *et al.* proposed a very complex formulation based on the flux splitting method (Pevchin *et al.*, 1997). In 1998, Yee tried to use the incompressible confinement term directly in the compressible flow equations; which lead to an unstable formulation (Yee, 1998). Finally, Hu *et al.* in 2002 proposed a stable formulation of vorticity confinement for the compressible flow equations (Hu *et al.*, 2002). Then, several studies have been conducted in this field. Among the recent works, the following researches can be mentioned: Sadri *et al.* used high-order fluxes along with the vorticity confinement method to solve the Euler equations in 2015 (Sadri *et al.*, 2015). O`regan *et al.* used the vorticity confinement method to simulate the airplane wingtip vortices. They used two methods of Unsteady Reynolds Averaged Navier-Stokes equations and LES for modeling the turbulent flow (O'Regan *et al.*, 2016). In 2016, Costes *et al.* proposed a vorticity confinement method with a 3-order accuracy, and used this method for Euler and Reynolds Averaged Navier-Stokes equations (M Costes *et al.*, 2016). In 2017, Petropoulos *et al.* increased the accuracy of this method to fifth order (Petropoulos *et al.*, 2017).

Despite the benefits of the vorticity confinement method, there is a fundamental problem in the way of generalization of this method. In order to get a correct solution, the confinement parameter must be specified by the user. Many efforts have been made to eliminate or mitigate this problem. In 2001, Lohner *et al.* presented an equation which related the value of the confinement parameter to the vorticity gradient (Lohner *et al.*, 2001). In 2003, Costes and Kowani proposed an equation that related the confinement parameter to local vorticity value (Michel Costes and Kowani, 2003). Robinson in 2004 correlated the value of the confinement parameter to helicity(Robinson, 2004). The research by Malek Jafarian and Pasandideh Fard in 2007 provided three confinement parameters (Jafarian and Fard, 2007). In 2008, Butsuntorn and Jameson proposed a formula relating the confinement parameter to the cell volume and helicity value (Butsuntorn and Jameson, 2008). In 2009, Han and Iaccarino introduced an equation for the confinement parameter using the difference in the results of upwind and central difference schemes(Hahn and Iaccarino, 2009). In addition, Bagheri Esfeh and Malek Jafarian in 2011, proposed a new method for calculating the confinement parameter (Bagheri-Esfeh and Malek-Jafarian, 2011). In spite of introduction of these schemes, the use of the vorticity confinement method still requires the

user involvement (in order to properly determine the confinement parameter). Another solution to solve the problem is to reduce the sensitivity of the results to the confinement parameter value. This issue was investigated by Pierson and Povitsky in 2013. Using TVD scheme, they could reduce the sensitivity of the results to the confinement parameter value (Pierson and Povitsky, 2013).

Despite the researches carried out in the field of vorticity confinement, a fundamental problem still remains. In this method, in most cases only the non-zero vorticity is the factor for vortex detection; therefore, the method is applied at each point of the solution domain where vorticity has a non-zero value. However, the vorticity value is not necessarily a reason for the existence of vortex. This causes an error in the results. In addition, it is worth noting that in conventional vorticity confinement formulation, computations are performed at all points of the domain, thus, part of the computational time and power is wasted. This problem can be solved somewhat by applying the non-zero vorticity condition; however, as noted above, the vorticity value cannot be used as a proper condition to detect the location of the vortices. Resolving this problem can increase the accuracy of the method and reduce the solution time. Therefore, it is necessary to investigate the effect of combining the vortex detection methods and vorticity confinement method.

Compared to other phenomenas (shocks, etc.), the definition of a vortex is more difficult. The center of the vortex can be related to areas of low pressure, low density and high vorticity. Moreover, this phenomenon is also known for its internal region structure. Due to these various features, different solutions are also provided for detection of the vortex. As a result, there is no comprehensive and single definition for the vortex. For example, a vortex can be considered as a ring whose surface has a constant velocity, however, this definition is not accurate for cases like shear and boundary layer flows. Especially when the local shear rate is equal to or greater than the vorticity rate. Nevertheless, in computational fluid dynamics (CFD) researches, the vorticity value is commonly used to define a vortex. Despite the relative efficiency of this definition, this can cause some problems (Kamkar *et al.*, 2009). Instead of using vorticity, a more comprehensive definition was described by Lugt in 1979, in which vortex is referred to as a set of material particles rotating around a common center (Lugt, 1979). The other method, known as the Q-criterion, was presented in 1988 by Hunt *et al.*. In this method, the parameter Q represents the difference between the local rotation and the shear strain rate (Hunt *et al.*, 1988). The method developed by Levy *et al.* in 1990 used the concept of helicity to detect vortex centers (Levy *et al.*, 1990). Helicity is the dot product of velocity and vorticity. Levy's method utilizes an eigenform of helicity which is non-dimensionalized by a function of velocity and vorticity and has a value in the domain of -1 to 1. In this method, it is assumed that the convective

motion of the particles in the vortex is in the direction perpendicular to the vorticity lines, so the values close to -1 and 1 represent the regions inside the vortex. While this method is very suitable for straight vortices, it is difficult to deal with curved vortices. Others, like Chong *et al.* (1990), used the eigenvalues of velocity gradient matrix. As, an imaginary root pair represents a rotating area. This method is often known as the Δ method, in which positive Δ values represent vortex. Δ is determined by the characteristic equation of the velocity gradient matrix (Chong *et al.*, 1990). Another approach based on the prediction-correction mechanism was proposed by Banks and Singer in 1994 to identify the vortex centers with more sensitivity (Banks and Singer, 1994). Another remarkable method was introduced by Sujudi and Haimes in 1995. This method was based on the critical point theory. In this method, the points with zero velocity and the indefinite streamline slope are considered as critical points (Sujudi and Haimes, 1995). In addition, Jong and Hussein developed a method called λ_2 in 1995. Their method is based on the eigenvalues of a matrix (indicator of the area with minimum pressure) (Jeong and Hussain, 1995). In 1999, Strawn *et al.* proposed a method of detecting a vortex core similar to the Sujudi method. In their method, the vortex center was detected by the local maximum vorticity (Strawn *et al.*, 1999). Horiuti and Takagi in 2005 created a method based on the detection of vortex sheets like structure rather than vortex tube like structure. Their method detects areas with large and continuous values of strain rate and rotation rate as vortex sheets. This method is known as the S Ω correlation method (Horiuti and Takagi, 2005). In 2009, Kamkar rewrote Q, λ_2, Δ and S Ω correlation methods as non-dimensional functions(Kamkar *et al.*, 2009).

So far, only the vorticity value has been used to determine the vortex in the vorticity confinement method. But this criterion dose not provides the correct result, in some cases, like shear layer and boundary layer flows. Considering the importance of correctly detecting vortex region, vortex feature detection methods have been used to determine these regions in this study by Combining the four vortex feature detection methods (Q, λ_2, Δ and S–Ω correlation) with vorticity confinement method, four new methods have been proposed. These methods and the conventional method are briefly referred to as $FD - CVC$ and CVC, respectively. These methods have been compared with CVC method in terms of solving time, sensitivity of the numerical solution to confinement parameter value, and oscillations. The results indicate a significant effect of $FD - CVC$ on the above cases.

2. GOVERNING EQUATIONS

In the present study, the combination of the compressible vorticity confinement method with two-dimensional Euler equation has been

investigated. Equation (1) shows this equation in the vector form.

$$\frac{\partial \overrightarrow{W}}{\partial t} + \frac{\partial \vec{F}}{\partial x} + \frac{\partial \vec{G}}{\partial y} = \vec{S} \tag{1}$$

In Eq. (1), $\overrightarrow{W}$ represents the vector of the flow quantities, in addition, $\vec{F}$ and $\vec{G}$ represent fluxes in x and y directions, respectively. These quantities have been shown in Eqs. (2), (3) and (4).

$$\overrightarrow{W} = \begin{bmatrix} \rho \\ \rho u \\ \rho v \\ \rho e_0 \end{bmatrix} \tag{2}$$

$$\vec{F} = \begin{bmatrix} \rho u \\ \rho u^2 + p \\ \rho v u \\ \rho u h_0 \end{bmatrix} \tag{3}$$

$$\vec{G} = \begin{bmatrix} \rho v \\ \rho v u \\ \rho v^2 + p \\ \rho v h_0 \end{bmatrix} \tag{4}$$

h_0 and p are calculated using Eqs. (5) and (6).

$$h_0 = e_0 + \frac{p}{\rho} \tag{5}$$

$$p = (\gamma - 1) \times \rho \times \left\{ e_0 - \frac{u^2 + v^2}{2} \right\} \tag{6}$$

In addition, $\vec{S}$ (source term) represents the compressible vorticity confinement (Eq. (7)).

$$\vec{S} = \begin{bmatrix} 0 \\ \rho \vec{f_b} . \hat{\imath} \\ \rho \vec{f_b} . \hat{\jmath} \\ \rho \vec{f_b} . \vec{V} \end{bmatrix} \tag{7}$$

One of the advantages of the vorticity confinement method is simplicity to adding it to the numerical solution, since the confinement term is added to the equations as a source term. This is true for incompressible and compressible problems. The confinement term acts in such a way that, according to Fig. 1 and Eq. (8), serves to convect $\overrightarrow{W}$ back towards the vortex center as it diffuses away. This convection must be in the direction perpendicular to the constant vorticity plane (in 3-D space) or constant vorticity lines (in 2-D space).
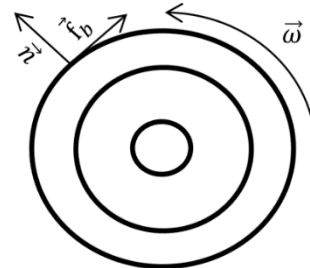

Fig. 1. vorticity confinement method

In the following, the terms of the source vector will be discussed further:

$$\vec{f_b} = -E_c \hat{n}_c \times \vec{\omega} \tag{8}$$

Where $\vec{f_b}$ terms are calculated as follow. The

vorticity value and its absolute magnitude are calculated in the solution domain, at first:

$$\vec{\omega}_z = \frac{\partial v}{\partial x} - \frac{\partial u}{\partial y} \tag{9}$$

$$\varphi = -|\vec{\omega}_z| = -\sqrt{\omega_z^2} \tag{10}$$

Then, the unit vector perpendicular to the vortex line is calculated using the gradient of the absolute vorticity.

$$\hat{n}_c = \frac{\vec{\nabla}\varphi}{|\vec{\nabla}\varphi|} = \varphi_{xs}\hat{\imath} + \varphi_{ys}\hat{\jmath} \tag{11}$$

Where, the values φ_{ys} and φ_{xs} are calculated through Eqs. (12) and (13).

$$\varphi_{ys} = \frac{-\varphi_y}{\sqrt{\varphi_x^2 + \varphi_y^2}} \tag{12}$$

$$\varphi_{xs} = \frac{-\varphi_x}{\sqrt{\varphi_x^2 + \varphi_y^2}} \tag{13}$$

By substituting from Eqs. (11) to (8) source terms of the momentum equations (Eq. (7)) are calculated in x and y directions as Eqs. (14) and (15).

$$\vec{f}_{bx} = -E_c \times (\vec{\omega_z}\varphi_{ys}) \tag{14}$$

$$\vec{f}_{by} = -E_c \times (\vec{\omega_z}\varphi_{xs}) \tag{15}$$

Which, E_c is called the confinement parameter and is responsible for controlling the value of the vorticity confinements term. On the other hand, by extending the Eq. (7), the vector of the source terms is rewritten as Eq. (16).

$$\vec{S} = \begin{bmatrix} 0 \\ \rho\vec{f}_{bx} \\ \rho\vec{f}_{by} \\ \rho(u\vec{f}_{bx} + v\vec{f}_{by}) \end{bmatrix} \tag{16}$$

The final form of the source term appears as Eq. (17), by substituting the Eqs. (14) and (15) in (16).

$$\vec{S} = \begin{bmatrix} 0 \\ -\rho E_c \vec{\omega}_z \varphi_{ys} \\ \rho E_c \vec{\omega}_z \varphi_{xs} \\ -\rho E_c \vec{\omega}_z (u\varphi_{ys} - v\varphi_{xs}) \end{bmatrix} \tag{17}$$

Despite the advantages of the vorticity confinement method, two major problems still remain. The first problem is related to determining the value of the confinement parameter, which must be adjusted with user intervention. The low values of this parameter cause the loss of the efficiency of the vorticity confinement. In addition, its excessive large value leads to oscillation and unrealistic results. In conventional methods, calculation of the vorticity confinement is performed throughout the solution domain, and hence, at each point of the solution domain where the vorticity has a value, this term has a value as well, since affects the solving process. This, in some cases, like boundary layer and shear layer flows, applies vorticity confinement in points outside the vortex. It can lead to errors in addition to increasing the computational load. The vortex

feature detection methods are based on the establishment of a threshold function. Performance of these methods are such that the points where the value of the threshold function is greater than a predetermined value is recognized as a vortex. Despite the difference among these methods, all of them somehow use a velocity gradient matrix (for a two-dimensional flow in accordance with Eq. (18)).

$$\nabla\vec{V} = \begin{bmatrix} \frac{\partial u}{\partial x} & \frac{\partial u}{\partial y} \\ \frac{\partial v}{\partial x} & \frac{\partial v}{\partial y} \end{bmatrix} \tag{18}$$

This matrix is divided into two symmetric and asymmetric parts S and Ω, respectively.

$$\nabla\vec{V} = S + \Omega \tag{19}$$

Equations (20 and 21) are used to calculate these matrices.

$$S = \frac{\nabla\vec{V} + (\nabla\vec{v})^T}{2} \tag{20}$$

$$\Omega = \frac{\nabla\vec{V} - (\nabla\vec{v})^T}{2} \tag{21}$$

In Eqs. (20) and (21), $\nabla\vec{V}^T$ represents the transposed velocity gradient matrix.

$$\nabla\vec{V}^T = \begin{bmatrix} \frac{\partial u}{\partial x} & \frac{\partial v}{\partial x} \\ \frac{\partial u}{\partial y} & \frac{\partial v}{\partial y} \end{bmatrix} \tag{22}$$

S and Ω are calculated, according to the Eqs. (23) and (24):

$$[S] = \begin{bmatrix} \frac{\partial u}{\partial x} & \frac{1}{2}\left(\frac{\partial u}{\partial y} + \frac{\partial v}{\partial x}\right) \\ \frac{1}{2}\left(\frac{\partial u}{\partial y} + \frac{\partial v}{\partial x}\right) & \frac{\partial v}{\partial y} \end{bmatrix} \tag{23}$$

$$[\Omega] = \begin{bmatrix} 0 & \frac{1}{2}\left(\frac{\partial u}{\partial y} - \frac{\partial v}{\partial x}\right) \\ \frac{1}{2}\left(\frac{\partial v}{\partial x} - \frac{\partial u}{\partial y}\right) & 0 \end{bmatrix} \tag{24}$$

The norm of matrix M is defined as Eq. (25).

$$\|M\| = [trace(MM^T)]^{\frac{1}{2}} \tag{25}$$

Square norm of matrices S and Ω are calculated as Eqs. (26) and (27).

$$\|S\|^2 = \left(\frac{\partial u}{\partial x}\right)^2 + \left(\frac{\partial v}{\partial y}\right)^2 + \frac{1}{2}\left(\frac{\partial u}{\partial y} + \frac{\partial v}{\partial x}\right)^2 \tag{26}$$

$$\|\Omega\|^2 = \frac{1}{2}|\vec{\omega}|^2 \tag{27}$$

2.1 Non-Dimensional Q Method

The Non-dimensional Q method is based on the vortex detection according to the norm value of matrices S and Ω. Hunt *et al.* established a relationship between these two matrices. They proposed the parameter Q in accordance with Eq. (28)(Hunt *et al.*, 1988).

$$Q = \frac{1}{2}(\|\Omega\|^2 - \|S\|^2) \tag{28}$$

By dividing the Eq. (28) into $\|S\|^2$, the Non-dimensional form is obtained as Eq. (29). The

resulting term is known as the threshold function and is calculated as follows(Kamkar *et al.*, 2009).

$$f_{threshold} = \frac{1}{2}\left(\frac{\|\Omega\|^2}{\|S\|^2} - 1\right) \qquad (29)$$

Since, according to Eq. (27), the term $\|\Omega\|^2$ denotes vorticity, its zero value will indicate lack of vorticity. Therefore, the threshold function tends to -0.5, in the areas outside the vortex.

$$f_{threshold} \rightarrow -\frac{1}{2} \qquad (30)$$

On the other hand, the high values of $\|\Omega\|^2$ indicates high intensity vorticity, in which the value of the threshold function tends to infinity.

$$f_{threshold} \rightarrow \infty \qquad (31)$$

In cases, like the boundary layer and the shear layer flows, again the value of the threshold function tends to -0.5, since the strain ($\|S\|^2$) is larger than vorticity ($\|\Omega\|^2$). Therefore these regions will not be identified as a vortex.

2.2 Non-dimensional λ_2 method

A low pressure region can represents the center of a vortex. In this case, the compressive force generated by this region is in equilibrium with a centrifugal force. However, in a non-rotating transient flow, it is also possible to create a low-pressure region. Therefore, it is not possible to determine the position of the vortex only by relying on the presence of a low pressure region. Nevertheless, Jong and Hussein used this feature of the vortex center as the basis to create a feature detection scheme. At first, they considered an incompressible Navier-Stokes equation(Jeong and Hussain, 1995). By simplifying and neglecting the viscosity, the transient strain, the material derivative of the velocity and density gradient, the equation turned into an eigenvector-eigenvalue problem as Eq. (32).

$$[S^2 + \Omega^2 - \lambda_i I]X_i = 0 \qquad (32)$$

In Eq. (32), X_i and λ_i represent the eigenvector and the eigenvalue, respectively. Negative eigenvalues indicate the presence of a low-pressure region on the plane specified with the corresponding eigenvector. Two negative eigenvalues will indicate the center of the vortex. $\lambda_2 < 0$ indicates the existence of a vortex, if three eigenvalues (three-dimensional problem) are considered as $\lambda_1 \leq \lambda_2 \leq \lambda_3$.

Like the threshold function defined in the non-dimensional Q method, also in this method, for ease of use in various problems, λ_2 was non-dimensionalized by the second norm of matrix S (Eq. (33)). The negative coefficient was applied in order to make the term positive in vortex region, (Kamkar *et al.*, 2009).

$$f_{threshold} = -\frac{\lambda_2}{\|S\|^2} \qquad (33)$$

2.3 Non-dimensional modified Δ method

Chong *et al.* provided a method similar to the λ_2 method, with the difference that the matrix is the velocity gradient matrix (Eq. (34)).

$$det[\nabla\vec{V} - \lambda I] = 0 \qquad (34)$$

This method leads to a third-order equation as Eq. (35), In 3D case (Chong *et al.*, 1990).

$$\lambda^3 + P\lambda^2 + Q\lambda + R = 0 \qquad (35)$$

Which, the values of P, Q and R are calculated in accordance with Eqs. (36) to (38).

$$P = -trace[\nabla\vec{V}] \qquad (36)$$

$$Q = \frac{1}{2}\left(P^2 - trace\left[\left(\nabla\vec{V}\right)^2\right]\right) \qquad (37)$$

$$R = -det[\nabla\vec{V}] \qquad (38)$$

It is worth noting that the Eq. (37) is identical with the definition in the Non-dimensional Q method. The solution of Eq. (35) yields to three real roots or one real root and two imaginary roots. The second case occurs when the value of Δ is positive according to Eq. (39).

$$\Delta = 4RP^3 - P^2Q^2 + 4Q^3 - 18PQR + 27R^2 > 0 \qquad (39)$$

In this case, the roots are as λ_r, $\lambda_{cr} \pm i\lambda_{ci}$. λ_c magnitude shows the rotational strength.. Therefore, it is used to define the threshold function (Eq. (40))(Kamkar *et al.*, 2009).

$$f_{threshold} = \frac{\lambda_{ci}}{\|S\|} \qquad (40)$$

It is worth noting that in this method, the norm of matrix S has been used for non-dimensionalization (contrary to the previous methods, which used the square of this parameter for non-dimensionalization).

2.4 S − Ω Correlation method

Unlike the previous methods, this method was designed to track the vortex sheet rather than the vortex tube. In this method, an eigenvalue problem is defined like Δ and λ_2 methods. Horiuti *et al.* proposed a eigenvalue problem as (Eq. (41))(Horiuti and Takagi, 2005).

$$[S\Omega + \Omega S - \lambda_i I]X_i = 0 \qquad (41)$$

According to this, the second answer (in terms of magnitude) is known as λ+ and the threshold function is defined as Eq. (42) (Kamkar *et al.*, 2009).

$$f_{threshold} = \frac{\lambda_+}{\|S\|^2} - 1 \qquad (42)$$

3. NUMERICAL SOLUTION METHOD

Equation (1) is integrated around each cell in the domain using the finite volume method and the central difference scheme. This leads to Eq. (43), which RHS is calculated in accordance with Eq. (44).

$$\vec{W}^{n+1} = \vec{W}^n + RHS \qquad (43)$$

$$RHS =$$

$$\frac{\Delta t}{\Delta x \times \Delta y}\left(\vec{F}_{i+\frac{1}{2}} - \vec{F}_{i-\frac{1}{2}} + \vec{G}_{j+\frac{1}{2}} - \vec{G}_{j-\frac{1}{2}} - AD\right) \qquad (44)$$

Equation (43) is solved by the fourth order explicit Runge-Kutta method as Eqs. (45-48)(Jameson *et al.*, 1981).

$$\vec{W}^0 = \vec{W}^n - \alpha_1 \text{RHS}(\vec{W}^n) \tag{45}$$

$$\vec{W}^1 = \vec{W}^n - \alpha_2 RHS(\vec{W}^0) \tag{46}$$

$$\vec{W}^2 = \vec{W}^n - \alpha_3 RHS(\vec{W}^1) \tag{47}$$

$$\vec{W}^{n+1} = \vec{W}^n - \alpha_4 RHS(\vec{W}^2) \tag{48}$$

The term AD (Eq. (44)) denotes the artificial viscosity fluxes added to the solution to eliminate oscillations and increase the stability. These fluxes are combinations of the second order terms to avoid oscillations, as well as the fourth order terms in order to increase stability. The time steps used in the solution are calculated locally at first, and then the smallest one is chosen as the time step in the entire domain of solution. The terms $\vec{W}^0$, $\vec{W}^1$, and $\vec{W}^2$ represent the values of $\vec{W}$ in the middle steps of the solution. Moreover, the Rung-Kutta coefficients are $\alpha_1 = \frac{1}{4}, \alpha_2 = \frac{1}{3}, \alpha_3 = \frac{1}{2}$, and $\alpha_4 = 1$.

4. PROBLEM DEFINITION

a single fixed vortex has been used as the case study in the present work. The domain is a square with dimensions of $1 \times 1\ m^2$. The initial conditions, was used in accordance with Povitsky and Ofengeim Eqs. (49) and (50) (Povftsky and Ofengeim, 1999).

$$U_\theta = \frac{R}{R_c} \qquad\qquad R < R_c \tag{49}$$

$$U_\theta = \frac{1}{R}\left(\frac{R_c^2 R_c}{R_o^2 - R_c^2}\right) - R\left(\frac{R_c}{R_o^2 - R_c^2}\right) R_c < R < R_o \tag{50}$$

Using the above equations, a single vortex, a combination of free vortex and forced vortex, was obtained according to Fig. 2 (R_c and R_o were considered as 0.05 and $10 \times R_c$, respectively).
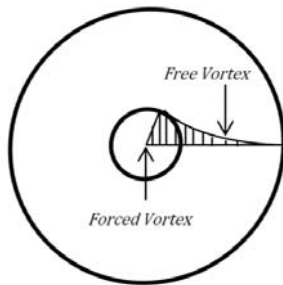
Fig. 2. Schematic of a single vortex

4.1 Solution Grid

The grid used in this study is a simple orthogonal grid of 100×100.

5. RESULTS

5.1 Vorticity Confinement Method

In the following, the combinations of the methods of Q, λ_2, Δ and $S - \Omega$ with the CVC method, are shown briefly with $FDQ - CVC$,

$FDL2 - CVC$, $FDD - CVC$, and $FDSO - CVC$, respectively. In the first step, the single vortex problem was investigated without applying the vorticity confinement method (briefly shown with W/CVC) to study the performance of the numerical solution code and the artificial viscosity. To compare, the velocity profiles were investigated on the vortex diameter for simplicity (Fig. 3).
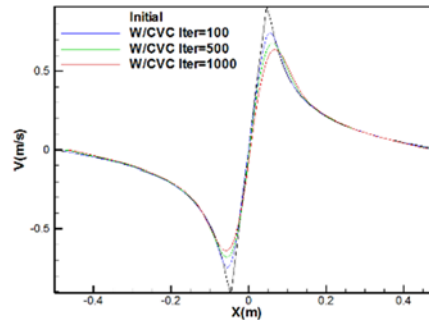

Fig. 3. Comparison of the initial velocity profile with the velocity profiles after 100, 500 and 1000 time steps (without vorticity confinement)

Since the problem under study is an inviscid flow, there must be no decrease in the velocity profile. However, according to Fig. 3, the velocity reduction is evident in the numerical solution. This is because of numerical discretization error. In the next step, the numerical solution of the vortex was performed using the confinement parameter of 0.001 (Fig. 4). It is observed that the application of the vorticity confinement method has improved the results. This improvement is not significant due to the very small amount of the confinement parameter ($E_c = 0.001$), however, the increase in the confinement parameter increases the effect of this method; this increase can leads to some problems. Figure 5 demonstrates the effects of using the excessive confinement parameter ($E_c = 0.1$). However, in addition to some oscillations, the maximum value of velocity is exceeds its initial value. These issues make the determination of the confinement parameter difficult. The vortex feature detection method can be used to solve these difficulties.
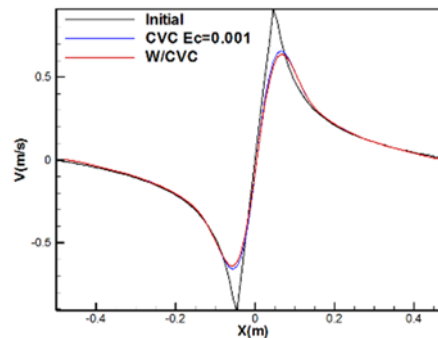

Fig. 4. Comparison of the initial velocity profile with the velocity profiles after 1000 time steps (with and without the vorticity confinement method)

5.2 Vortex Feature Detection Methods

In the present study, four feature detection methods, described in 2, have been used. The results are as follow (Fig. 6). It can be seen that despite the precision used in the feature detection
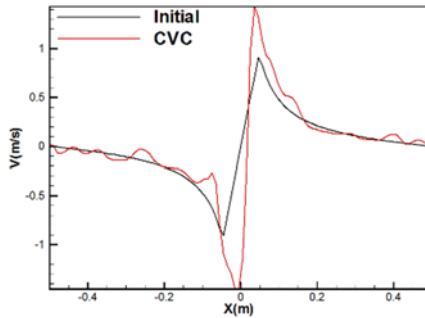

Fig. 5. Comparison of the initial velocity profile with the velocity profile after 1000 time steps (using the confinement parameter 0.1)

methods, still, points outside the vortex region are also marked as vortices. To remove these points, the filtering operation had to be performed. In the non-dimensional Q method, this process was performed as follows. In the first step, a criterion was defined for maximum error as Eq. (51).

$$\overline{S}_{noise} = \frac{k}{100} Q_{max} \qquad (51)$$

Where, the value of k was 0.01. Finally, any point where the value of the parameter Q is less than $\overline{S}_{noise}$, was considered to be outside the vortex. The results can be seen in Fig. 7. The question is, whether the size of the mesh can affect the results or not. Figure 8 shows the results of the non-dimensional Q method with different numerical solution grids (after filtering).
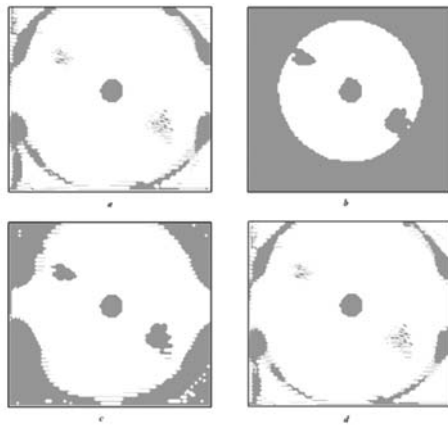
Fig. 6. Locus of the vortex obtained from the a) non-dimensional Q, b) λ_2, c) Δ, d) $S - \Omega$ methods (Before filtering)

The surfaces detected as a vortex, decreases as the number of grids are increased. However, the rate of this decrease is reduced by decreasing the mesh size so that the difference between the results of the 100 * 100 and 150 * 150 grids is much less than the difference between those of

the 30 * 30 and 50 * 50. As in any case, at least 70% of the vortex surface was covered. Therefore, the size of the solution grid can be ignored. As noted above, the vorticity confinement method is ineffective in lower values of the confinement parameter In addition, oscillations occur that produce non-physical flows at higher values of parameter. In addition to generating errors, applying this method to locations outside the vortex leads to waste of time. Vortex feature detection methods can overcome these difficulties, partially. This will discuss in the next section.
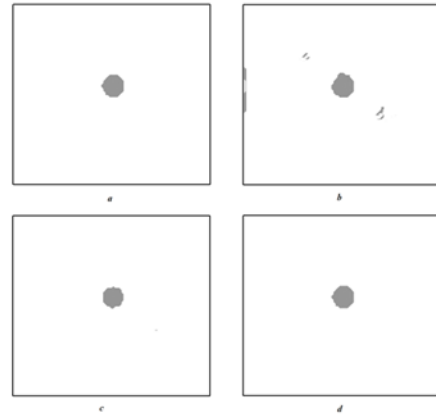

Fig. 7. Locus of the vortex obtained from the a) non-dimensional Q, b) λ_2, c) Δ, d) $S - \Omega$ methods (After filtering)
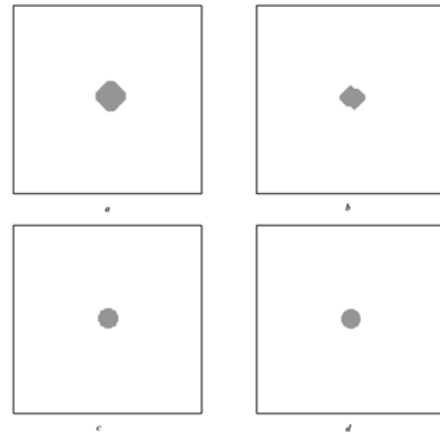

Fig. 8. Locus of the vortex obtained from the non-dimensional Q method in a solution grid of a) 30 * 30 b) 50 * 50, c) 100 * 100, d) 150 * 150

5.3 Investigation of the Effect of Combination of Vorticity Confinement Method with Vortex Feature Detection Methods

In order to investigate the effect of combination of vortex feature detection and vorticity confinement methods, the results were compared with conventional method. This comparison was performed for three values of

the confinement parameter (0.001, 0.01, and 0.1) (Figs. 9 to 11). Using the lowest value of parameter (0.001), in general, the results are close to each other in all five cases (Fig. 9). But when the value increases to 0.01, the difference between the results of the CVC method and the $FD-CVC$ methods is significant. Nevertheless, the $FD-CVC$ methods still offer an acceptable value (Fig. 10). The over-confinement is evident in the results of the CVC and $FDL2-CVC$ methods, with further increase in the confinement parameter ($E_c = 0.1$), (Fig. 11). Both methods give similar results in terms of maximum velocity, however, oscillations are observed outside of the vortex core when using the CVC method. But all $FD-CVC$ methods are oscillation free. In addition, except for the $FDL2-CVC$ method, other methods still present acceptable results. It can be said that these methods have somehow resisted the over-confinement and oscillation errors (Fig. 11). To better understand the effect of the suggested $FD-CVC$ methods in the present work, their results were compared with the results of the CVC method (Figs. 12 to 16). Figures 12 to 16 represents the velocity profile of single vortex, derived from CVC and FD-CVC methods using confinement parameters of 0.001, 0.01 and 0.1. It can be seen that increasing the confinement parameter (using CVC method), the maximum velocity increases and it exceeds the initial maximum one at the value of 0.1 (Fig. 12). Also some oscillations occur at this value. In contrast, increasing the confinement parameters in FD-CVC methods do not lead to oscillation (Figs. 13 to 16). In addition, maximum velocity does not exceed its initial value using FD-CVC methods, except FDL2-CVC method (Fig. 14) . Another interesting point is that the results of FDQ-CVC and FDD-CVC methods (Figs. 13 and 15) show the rate of increase in maximum

velocity is reduced by increasing the confinement parameter value. Therefore, it can be concluded that, generally FD-CVC methods are less dependent on the value of confinement parameter than the original method and they have reduced the negative effects of high values on the results .
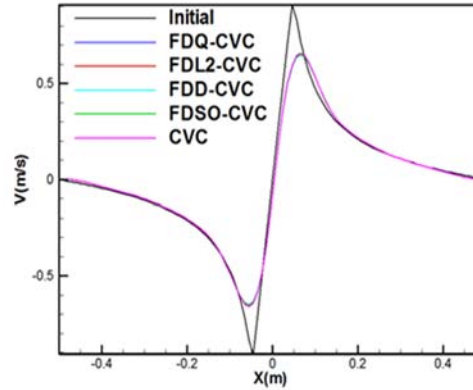

Fig. 9. Comparison of the initial velocity profile with the velocity profiles derived from CVC method and the FD-CVC methods using the confinement parameter of 0.001 after 1000 time steps

figure 17 shows the changes in the maximum velocity magnitude during 10000-time steps, using FDQ-CVC, CVC and without CVC. Small values of Ec (0.001) leads to decrease of velocity magnitude over time. CVC method results in over confinement but FDQ-CVC leads to a steady-state solution, Using Ec=0.01. Using large value of confinement parameter (Ec=0.1), CVC method suffers from severe oscillations. On the other hand, maximum mean velocity Converges over time to steady-state solution using FDQ-CVC method.
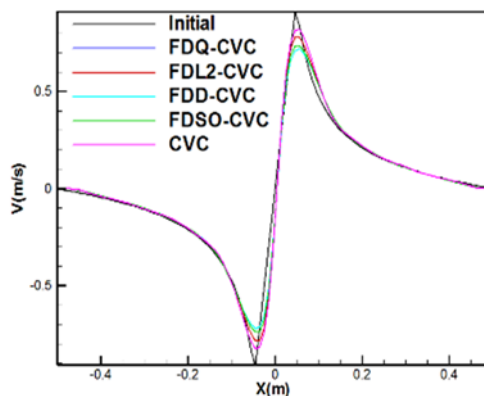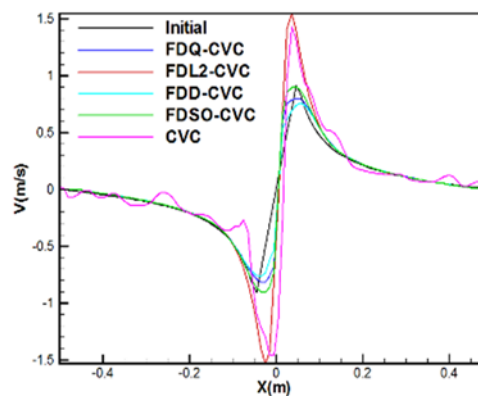

Fig. 10. Comparison of the initial velocity profile with the velocity profiles derived from CVC method and the $FD-CVC$ methods using the confinement parameter of 0.01 after 1000 time steps

Fig. 11. Comparison of the initial velocity profile with the velocity profiles derived from CVC method and $FD-CVC$ methods using the confinement parameter of 0.1 after 1000 time steps
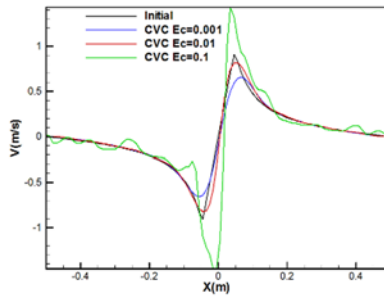
Fig. 12. Comparison of the initial velocity profile with the velocity profiles derived from CVC method using the confinement parameters 0.001, 0.01 and 0.1 after 1000 time steps
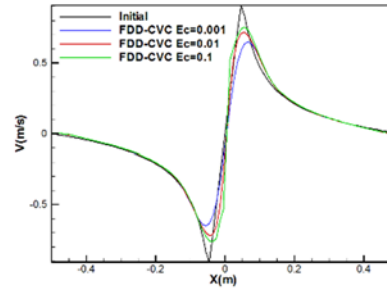

Fig. 13. Comparison of the initial velocity profile with the velocity profiles derived from $FDQ - CVC$ method using the confinement parameters 0.001, 0.01 and 0.1 after 1000 time steps
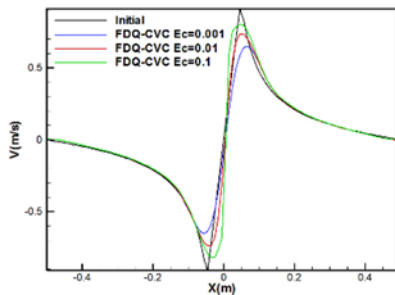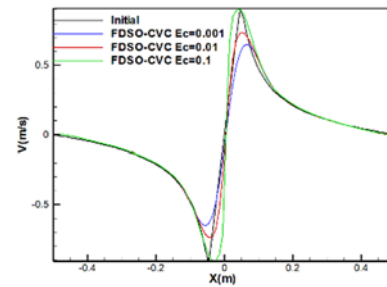

Fig. 14. Comparison of the initial velocity profile with the velocity profiles derived from $FDL2 - CVC$ method using the confinement parameters 0.001, 0.01 and 0.1 after 1000 time steps
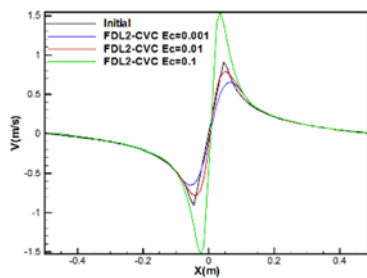

Fig. 15. Comparison of the initial velocity profile with the velocity profiles derived from $FDD - CVC$ method using the confinement parameters 0.001, 0.01 and 0.1 after 1000 time steps

Fig. 16. Comparison of the initial velocity profile with the velocity profiles derived from $FDSO - CVC$ method using the confinement parameters 0.001, 0.01 and 0.1 after 1000 time steps
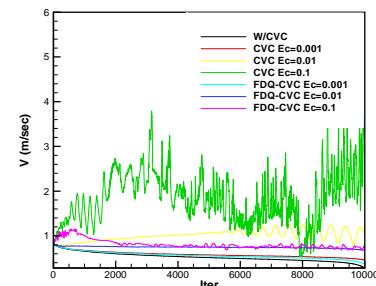

Fig. 17. Variation of maximum velocity vs. time steps for CVC and FDQ-CVC methods with different confinement parameters

5.4 Comparison of the Classical Method and the Combined Method in Separate Meshes

Less sensitivity and lack of oscillation errors in the $FD - CVC$ methods can provide another opportunity to save time. Similar result or better one, on a fine grid, can be obtained than the one using coarse grid with large confinement parameter. In Fig. 18, the comparison of the velocity profile derived from the CVC method on a 100×100 grid with the result of the $FDL2 - CVC$ method on a 60×60 grid ($E_c = 0.08$) is shown that the results are similar. It`s worth noting that, this trick is not possible for CVC method due to oscillations (Fig. 18).

5.5 ANALYSIS OF THE ERROR DIFFUSION PROCESS IN THE VORTICITY CONFINEMENT METHOD

One of the advantages of the FD-CVC methods is the lack of oscillation in velocity profiles at high values of the confinement parameter. To analysis this, the vorticity contours obtained by the FDQ-CVC method was compared with similar results of CVC method (Figs. 21 and 22). When using FDQ-CVC method, the vorticity contours are not observed outside the vortex core, and the vortex retains its circular shape (Fig. 19). But, the entire domain filled with several vortices and the vortex has lost its natural shape, using CVC (Fig. 20). To understand why this happens,
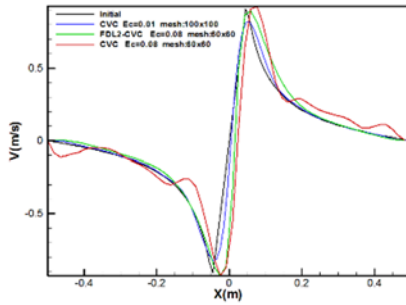
Fig. 18. Comparison of the initial velocity profile with the velocity profile obtained by the CVC method using the confinement parameter 0.01 on a 100×100 solution grid, the CVC method using the confinement parameter 0.08 on a 60×60 solution grid, and the $FDL2 - CVC$ method using the confinement parameter 0.08 on a 60×60 solution grid, after 1000 time steps

the vorticity contours were plotted in time steps of 100, 200, 300, and 400 using the CVC method (Fig. 21). According to Fig. 3, the vortex in this problem consists of two sections, free and forced, the vorticity value is zero in the free section (R>R_C). But it was observed that at the beginning due to a numerical error, vorticity has a value in the free vortex section, and these regions grow with time (Fig. 23). The reason for this phenomenon can be explained as the vorticity confinement method has been created as a way to compensate for the errors caused by numerical solutions. However, this method can never completely prevent numerical errors. Therefore, this method has the potential to add an error to numerical
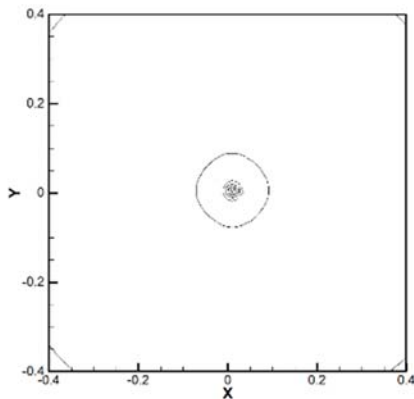
solution. In such a way that, at each time step, small errors are created as unrealistic values of vorticity. In the next step, since the only factor of application of confinement term is the vorticity value, hence, artificial vortices are also mistakenly influenced by the vorticity confinement method. Therefore, the small errors normally disappeared due to the diffusion process, are maintained and amplified by vorticity confinement. This will be repeated in the next time steps. As a result, the errors increase. This is more evident especially at high confinement parameter values (here 0.1) or large solution times. the $FD - CVC$ method can be effective In this case. If the numerical errors bring unrealistic values of vorticity in the solution domain; since the feature detection method does not allow applying vorticity confinement at these points, the error is not amplified and the artificial vortices will be eliminated. Therefore, the numerical solution will be largely free of the oscillation in the $FD - CVC$ methods.

5.6 Investigation of the Effect of $FD - CVC$ Methods on the Solution Time

As stated previously, vorticity confinement uses vorticity for recognition of vortex region. The presence of vorticity alone is not a reason for the existence of a vortex. This can lead to errors in the numerical solution. Furthermore, the calculations of vorticity confinement outside the vortex regions increase calculation time. Therefore, a method is required which detects the vortex regions from non-vortex ones and apply the vorticity confinement method at right
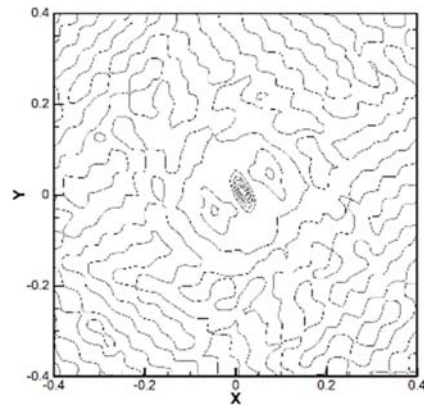

Fig. 19. Vorticity contours obtained by the $FDQ - CVC$ method using the confinement parameter of 0.1 after 1000 time steps

Fig. 20. Vorticity contours obtained by the CVC method using the confinement parameter of 0.1 after 1000 time steps

places (FD-CVC), which is the subject of the present study. In addition to preventing errors, this method can increase the speed of numerical solution. The effectiveness of the FD-CVC methods can greatly depend on part of the solution domain occupied by the vortex. So this issue has been considered in the investigations. To evaluate this effect, the problem of a single vortex has been considered. The first step of calculating the solution time is, preforming vorticity confinement

all over the domain and recording time for these calculations (CVC method). Then, the vortex area is specified each time by a vortex feature detection method and vorticity confinement is performed in that area (FD-CVC methods). This process is repeated 10,000 times in the present study. Finally, average amount of time spent for a time step is compared among five methods. To study the effect of vortex center dimension (Rc) to the solution domain (L) ratio, these calculations have been

performed for four values of (Rc/L). The results (Fig. 22) indicate the fact that in most of Rc/L values, the proposed combined methods performed the vorticity confinement in less time. Only in high values of this parameter, the use of these methods is not associated with time saving (which is rare in practical applications). It was also observed that FDQ-CVC has the fastest solution, followed by FDL2-CVC in the second place, and finally the FDSO-CVC and FDD-CVC. It is worth noting that the reported values correspond to a 100 × 100 grid, which is only for a single time step, and the difference is more evident with the smaller grids.
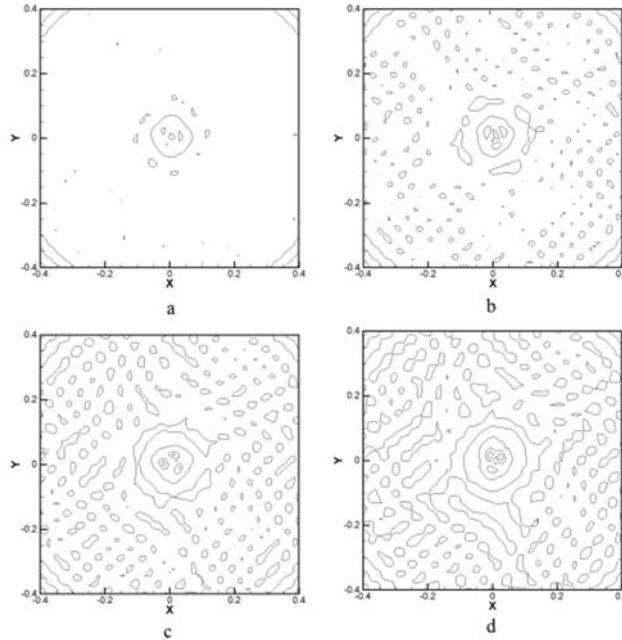

Fig. 21. Vorticity contours obtained by the CVC method using the confinement parameter of 0.1 after a) 100, b) 200, c) 300, and d) 400 time steps
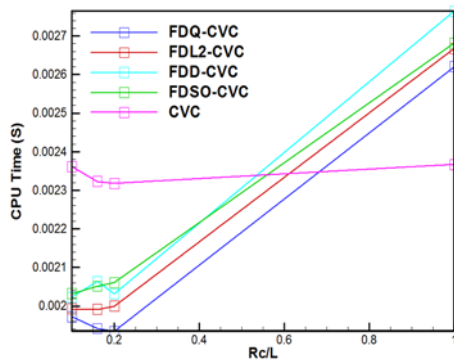

Fig. 22. Comparison of solution time on 100×100 grid for different methods

6. CONCLUSION

In the present study, the combination of compressible vorticity confinement method with the vortex feature detection methods was proposed to limit the effect of vorticity confinement on vortex regions. The following results were obtained for the non-viscous compressible flow of a single vortex with a Mach number of 0.5:

- All $FD - CVC$ methods have higher solution speed than the CVC in real conditions.

- The sensitivity of the results to the confinement parameter value is reduced using three $FDQ - CVC$, $FDD - CVC$, and $FDSO - CVC$ methods.
- All $FD - CVC$ methods show higher resistance to oscillation compared to CVC. This property allows achieving results similar to those of a finer grid, using high values of confinement parameter on coarse ones. This capability is limited in CVC method due to the occurrence of oscillations at high values of confinement parameter.

REFERENCES

Bagheri-Esfeh, H. and Malek-Jafarian, M. (2011). Development of artificial dissipation schemes and compressible vorticity confinement methods. Proceedings of the Institution of Mechanical Engineers, Part G: *Journal of Aerospace Engineering* 225(8), 929-945.

Banks, D. C. and Singer, B. A. (1994). *Vortex tubes in turbulent flows: identification, representation, reconstruction. Visualization*, 1994., Visualization'94, Proceedings., IEEE Conference on, 132-139

Butsuntorn, N. and Jameson, A. (2008). *Time*

spectral method for rotorcraft flow. 46th AIAA Aerospace Sciences Meeting and Exhibit, 2008-0403.

Chong, M. S., Perry, A. E. and Cantwell, B. J. (1990). A general classification of three-dimensional flow fields. *Physics of Fluids A: Fluid Dynamics* 2(5), 765-777.

Costes, M. and Kowani, G. (2003). An automatic anti-diffusion method for vortical flows based on Vorticity Confinement. *Aerospace Science and Technology* 7(1), 11-21.

Costes, M., Petropoulos, I. and Cinnella, P. (2016). Development of a third-order accurate vorticity confinement scheme. *Computers & Fluids* 136, 132-151.

Hahn, S. and Iaccarino, G. (2009). *Towards adaptive vorticity confinement*. 47th AIAA Aerospace Sciences Meeting and Aerospace Exposition, 2009-1613

Horiuti, K. and Takagi, Y. (2005). Identification method for vortex sheet structures in turbulent flows. *Physics of Fluids* 17(12), 121703.

Hu, G., Grossman, B. and Steinhoff, J. (2002). Numerical method for vorticity confinement in compressible flow. *AIAA journal* 40(10), 1945-1953.

Hunt, J. C., Wray, A. A. and Moin, P. (1988). *Eddies, streams, and convergence zones in turbulent flow*s.

Jafarian, M. M. and Fard, M. P. (2007). Development and application of compressible vorticity confinement. *Scientia Iranica* 14(3), 251-262.

Jameson, A., Schmidt, W. and Turkel, E. (1981). Numerical solutions of the Euler equations by finite volume methods using Runge-Kutta time-stepping schemes. AIAA paper 1259, 1981.

Jeong, J. and Hussain, F. (1995). On the identification of a vortex. *Journal of fluid mechanics* 285, 69-94.

Kamkar, S., Jameson, A. and Wissink, A. M. (2009). *Automated Grid Refinement Using Feature Detection*. 47th AIAA Aerosciences Conference, 2009-1496

Levy, Y., Degani, D. and Seginer, A. (1990). Graphical visualization of vortical flows by means of helicity. AIAA journal 28(8), 1347-1352.

Lohner, R., Yang, C. and Roger, R. (2001). *Tracking vortices over large distances using vorticity confinement*. ECCOMAS CFD,

Lugt, H. J. (1979). *The dilemma of defining a vortex*. Springer Berlin, Heidelberg,

O'Regan, M., Griffin, P. and Young, T. (2016). A vorticity confinement model applied to URANS and LES simulations of a wing-tip vortex in the near-field. *International Journal*

of Heat and Fluid Flow 61, 355-365.

Petropoulos, I., Costes, M. and Cinnella, P. (2017). *Development and analysis of high-order vorticity confinement schemes. Computers & Fluids.*

Pevchin, S. V., Steinhoff, J. and Grossman, B. (1997). *Capture of contact discontinuities and shock waves using a discontinuity confinement procedure*. AIAA paper (97-0874).

Pierson, K. and Povitsky, A. (2013). *Vorticity Confinement technique for preservation of tip vortex of rotating blade*. 31st AIAA Applied Aerodynamics Conference, 2420

Povftsky, A. and Ofengeim, D. (1999). Numerical study of interaction of a vortical density inhomogeneity with shock and expansion waves. *International Journal of Computational Fluid Dynamics* 12(2), 165-176.

Robinson, M. (2004). *Application of vorticity confinement to inviscid missile force and moment prediction*. 42 nd AIAA Aerospace Sciences Meeting 717.

Sadri, M., K. Hejranfar, and M. Ebrahimi (2015). On application of high-order compact finite-difference schemes to compressible vorticity confinement method. Aerospace Science and Technology 46, 398-411.

Steinhoff, J. (1994). Vorticity confinement: A new technique for computing vortex dominated flows. *Frontiers of Computational Fluid Dynamics*, 235-263.

Steinhoff, J., Mersch, T. and Decker, F. (1994). *Computation of incompressible flow over delta wings using vorticity confinement*. 32nd Aerospace Sciences Meeting and Exhibit, 646

Steinhoff, J. and Raviprakash, G. (1995). *Navier-Stokes computation of blade-vortex interaction using vorticity confinement*. 33rd Aerospace Sciences Meeting and Exhibit, 161

Steinhoff, J., Wang, C., Underhill, D., Mersch, T. and Wenren, Y. (1992). *Computational vorticity confinement: A non-diffusive Eulerian method for vortex-dominated flows*. preprint, UTSI, Tullahoma, TN.

Steinhoff, J., Wenren, Y., Underhill, D. and Puskas, E. (1995). *Computation of short acoustic pulses. Proceedings, 6th International Symposium on CFD*, Lake Tahoe NV, Sept,

Strawn, R. C., Kenwright, D. N. and Ahmad, J. (1999). Computer visualization of vortex wake systems. *AIAA J* 37(4), 511-512.

Sujudi, D. and Haimes, R. (1995). *Identification of swirling flow in 3D vector fields.*

Yee, K. (1998). *An Euler calculation for a hovering coaxial rotor flow field with new*. 24 th European Rotorcraft Forum.